The Effect of Clustered Scatterers on Volume Reverberation

Tom Weber
Center for Coastal and Ocean Mapping, 24 Colovos Road
University of New Hampshire
Durham, NH 03284
phone: (603) 862-1659 fax: (603) 862-0839 email: weber@ccom.unh.edu

Award Number: N0014-09-1-0575
http://marine.unh.edu/people/faculty/weber-tom.html

LONG-TERM GOALS

The long term goal of this work is to further the understanding of how clustering in clouds of discrete scatterers has an effect on both forward propagating and backscattered acoustic fields. Clustering is considered to be present when there are spatially dependent correlations in the fluctuating positions of the scatterers. For example, bubble clouds created by oceanic breaking waves have been observed to exhibit clustering at a level that would have a significant impact on the forward propagating acoustic field. Clustering may also be present in fish aggregations (e.g., nearest neighbor distances, school morphologies driven by behavior, inter-school spacing), and should be considered when examining bioclutter. This work is based on a) refining theoretical approaches so that they include clustering; and b) observing clustering in the important classes of discrete volume scatterers in the ocean.

OBJECTIVES

This objectives of this research are to 1) further develop the basic constructs that have previously been used for examining clustering amongst bubbles so that it can be used to examine reverberation caused by clustering in fish aggregations at mid- to low-frequencies (i.e., at or near swim bladder resonances), and 2) leverage existing fisheries high resolution multibeam sonar data collection efforts (or other similar efforts) to look for clustering within, or between, aggregations of fish, and to then to predict the effect of this clustering on volume reverberation.

APPROACH

This work seeks to extend the previous work examining clustering in clouds of bubbles [Weber et al. 2007, Weber 2008] by looking specifically at backscatter and volume reverberation from schools of fish. A modeling component used previously by Weber et al. [2007], which is based on the multiple scattering work of Foldy [1945], examines acoustic fields in free-space (i.e., short range or deep water scenarios). This has been modified to work with small schools of fish where the number of scatterers is far less than what would be found in most clouds of bubbles, making direct simulation of the full multiple scattering series a possibility. Key questions are related to if or when multiple scattering becomes important or, conversely, when the simpler single scattering solutions adequately describe the acoustic backscattered field.

Report Documentation Page

Form Approved
OMB No. 0704-0188

1. REPORT DATE	2. REPORT TYPE	3. DATES COVERED
SEP 2011		**00-00-2011 to 00-00-2011**

4. TITLE AND SUBTITLE	5a. CONTRACT NUMBER
The Effect of Clustered Scatterers on Volume Reverberation	5b. GRANT NUMBER
	5c. PROGRAM ELEMENT NUMBER
6. AUTHOR(S)	5d. PROJECT NUMBER
	5e. TASK NUMBER
	5f. WORK UNIT NUMBER
7. PERFORMING ORGANIZATION NAME(S) AND ADDRESS(ES) **University of New Hampshire,Center for Coastal and Ocean Mapping,24 Colovos Road,Durham,NH,03284**	8. PERFORMING ORGANIZATION REPORT NUMBER
9. SPONSORING/MONITORING AGENCY NAME(S) AND ADDRESS(ES)	10. SPONSOR/MONITOR'S ACRONYM(S)
	11. SPONSOR/MONITOR'S REPORT NUMBER(S)

12. DISTRIBUTION/AVAILABILITY STATEMENT
Approved for public release; distribution unlimited

13. SUPPLEMENTARY NOTES

14. ABSTRACT

15. SUBJECT TERMS

16. SECURITY CLASSIFICATION OF:			17. LIMITATION OF ABSTRACT	18. NUMBER OF PAGES	19a. NAME OF RESPONSIBLE PERSON
a. REPORT	b. ABSTRACT	c. THIS PAGE			
unclassified	**unclassified**	**unclassified**	**Same as Report (SAR)**	**10**	

In addition, existing high frequency multibeam sonar data along with aerial imagery have being leveraged to look for clustering within aggregations of juvenile Atlantic bluefin tuna (ABT, *Thunnus thynnus*) in order to create a realistic simulation of bioclutter. ABT represent a highly mobile, fast traveling schooling fish found throughout both the western and eastern Atlantic [Gibbs and Collette, 1966]. We specifically look at the morphology and spatial ordering observed in ABT observed in August 2009 (data collected as part of a separately funded project in collaboration with Molly Lutcavage, then with the UNH Large Pelagics Research Center, and processed in part by Maddie Schroth-Miller, a graduate student at UNH). This high resolution data, in which individuals can be resolved, is used in both single- and multiple-scattering models to simulate/examine the effects of spatial ordering on mid-frequency backscatter from the school, using a similar (but extended) methodology to that described by Weber et al. [2007].

WORK COMPLETED

Creation of a school model based on high frequency multibeam and aerial imagery data

Existing observations of juvenile ABT schools have been mined in order to create a 'kernel' for generating realistic synthetic schools. These data include both side-looking multibeam data (Figure 1a), which provides a vertical slice through the school, and aerial imagery which provides a horizontal image of the school (Figure 1b).

The multibeam data were processed to isolate the backscatter from the ABT using a constant false alarm rate (CFAR) approach with a threshold chosen on a pixel by pixel (i.e., each range/angle bin) noise history of data with no ABT present. After thresholding, the resulting data subset was despeckled, obvious outliers were manually removed, and the final result was considered to be a representation of a school cross-section. In order to determine an average cross-sectional shape, a convex hull was defined for each cross section and used to extract a school shape (Figure 2). The school shape is defined as the convex hull averaged over 10's of independent multibeam pings. For the purpose of this study, the school shape was simplified to an ellipse with the same average shape parameter (the circumference divided by the area).

The aerial imagery data were manually classified to identify individual fishes (Figure 3), and both the location (center of mass) and fish bearing (relative to the image coordinates) were estimated for each fish. Several images (corresponding to the same school) were then combined in order to estimate the positional dependency of the nearest neighbors for each fish, with the result shown in Figure 4.

The aerial imagery data indicate that the nearest neighbor is, on average, approximately 0.5 body lengths away and is preferentially located at a relative bearing (orientation relative to the swimming direction of the original fish) of approximately +/-45º or +/-135 º. In order to determine whether the apparent preferred bearings to neighboring fish are statistically significant (or, conversely, are artifacts of the low-pass filtering), a Kolmogorof-Smirnov test was used to determine if the bearings for each of the nearest neighbors (1^{st} through 6^{th}) fit a uniform distribution. This hypothesis was rejected at the 5% significance level only for the nearest neighbor, as expected, and also, unexpectedly, for the sixth neighbor. Apart from the unexplained 6^{th} neighbor, this is an indication that the tuna can be adequately modeled as pairs. As a (partial) test of this assertion, a bootstrapping method was used to simulate the aerial imagery data using only the low-passed filtered 2D histogram for the nearest neighbor, with the result shown in Figure 6. The simulation result appears qualitatively similar to the empirically derived 2D histograms shown in Figure 4.

Together, the data parameterizing the ABT schools (horizontal shape, vertical shape, nearest neighbor parameterizations) that has been extracted from the multibeam data and aerial imagery are used to simulate realistic fish distributions. This has been done with varying levels of spatial order including 1) no spatial order (Poisson distributed); 2) a nearest neighbor criteria in range only; and 3) a nearest neighbor criteria governing both range and relative bearing.

Modeled acoustic propagation through simulated Atlantic bluefin tuna schools

Bluefin tuna are slightly more dense than seawater and utilize a gas-filled swim bladder to maintain swimming depths at slow speeds [Magnuson, 1973]. The swim bladder, which has a size dependent mechanical resonance, is expected to dominate the acoustic response at low-mid frequencies. Although it is known that the swim bladder of individual tuna are highly variable in both their shape and size [Gibbs and Collette, 1966], no metrics describing this variability appear to be available in the published literature. For the purposes of this work, which is designed to match observations of 80-100 cm size bluefin tuna, a swim bladder volume of 250 cc was used based on the work of Schaeffer and Oliver [1999] who examined the swim bladder of yellowfin tuna (*Thunus albacores*). Despite the possible difference between species, this is thought to be a reasonable approximation given that both species would have needed to develop a swim bladder for the same mechanical reasons outlined by Magnuson [1973]. The 250 cc swim bladder volume corresponds approximately to a 100 cm length juvenile tuna. The target strength for an individual tuna (swim bladder) of this size was estimated using the model described by Love [1978].

Two acoustic models are examined here for random realizations of school models containing 263 fish (the number of fish observed in the aerial imagery underlying the model):

1) A coherent single scattering approximation, $|\sum_i p_o s_i G(r, r_i)|^2$, in which both the effect of the depth of the tuna and its relative distance from a monostatic sonar are considered.
2) A coherent multiple scattering approximation, $\left|\sum_i p^i s_i G(r, r_i)\right|^2$, which is similar to the second model but is exact for a given realization of point scatterers.

where p_o is the incident field at the fish accounting only for the direct path from the sonar, p^i is the incident field at the fish accounting for the direct path as well as contributions from each other fish, s_i is the complex scattering amplitude of the i^{th} fish, and G describes the free-space Greens function between the fish and the receiver (assumed here to be collocated with the source so that we are looking at backscatter).

Backscatter from the various types of simulated schools of ABT was then generated using a Monte Carlo simulation (N=5000) at frequencies ranging from a few 10's of Hz to 5 kHz. The output of the model are ensembles of complex backscattered pressure as would be observed by low-mid frequency monostatic sonar.

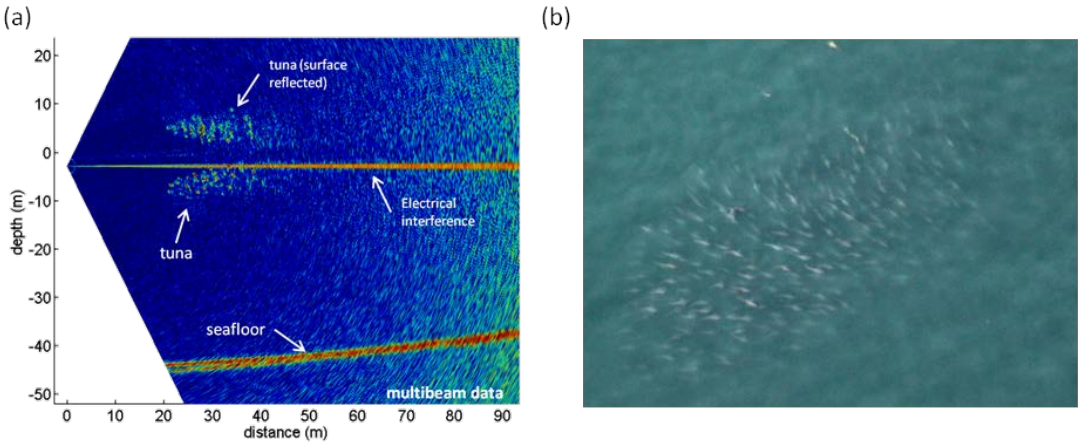

Figure 1. (a) 400 kHz side-looking multibeam data showing a vertical cross-section of an Atlantic bluefin tuna (ABT) school. (b) Aerial imagery of a similar ABT school.

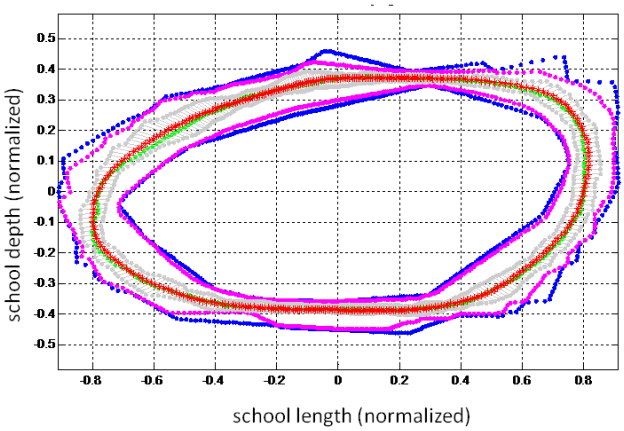

Figure 2. An example of the normalized average school shape (red line) extracted from a subset of the multibeam data. The school length and school depth are normalized by the square root of the school area. The blue, magenta, and grey lines indicate the max/min, 10^{th}/90^{th} percentiles, and 25^{th}/75^{th} percentiles of the school shape, respectively.

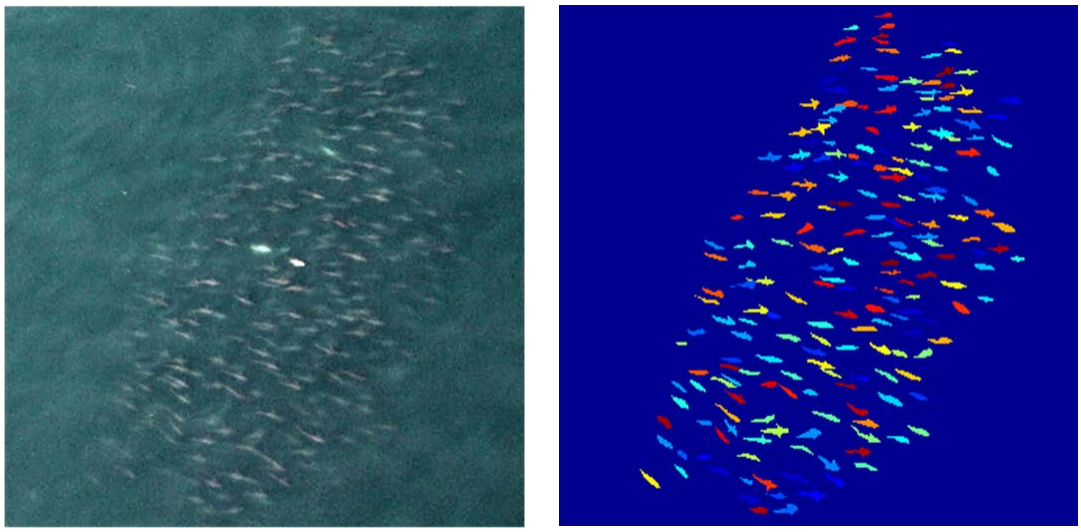

Figure 3. An example of the aerial imagery of the ABT schools. The raw image is shown on the left, the classified image is shown on the right.

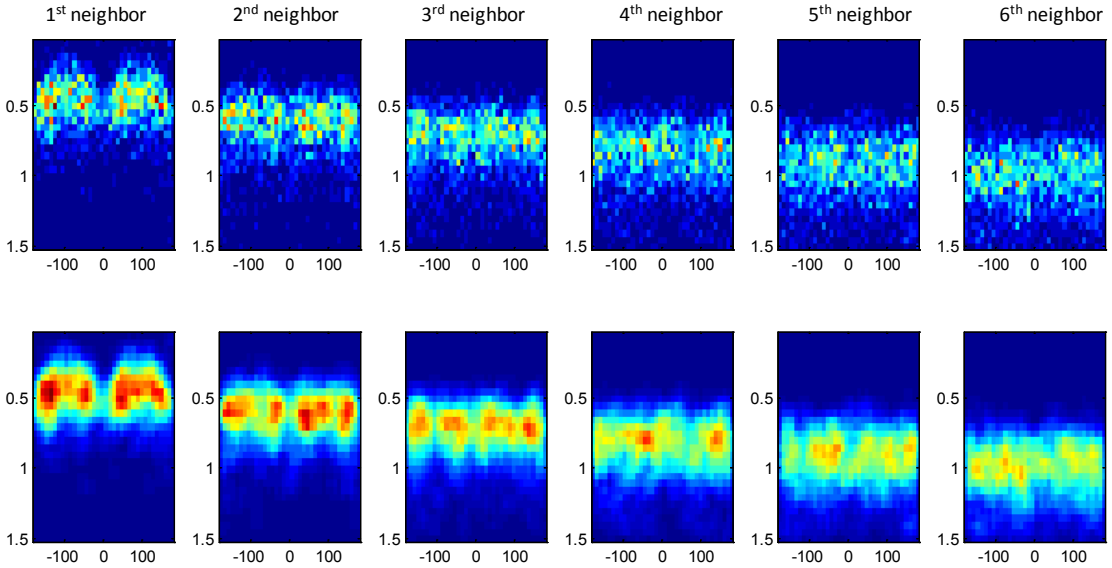

Figure 4. 2D histograms describing the positional dependency of the nearest neighbors of an individual tuna, plotted as a function of relative bearing (+/- 180 degrees) and range (# body lengths). The first column represents the nearest neighbor, the second column represents the next closest neighbor, and so on. The top row shows the raw histogram, and the bottom row shows a low-pass filtered version of the histogram.

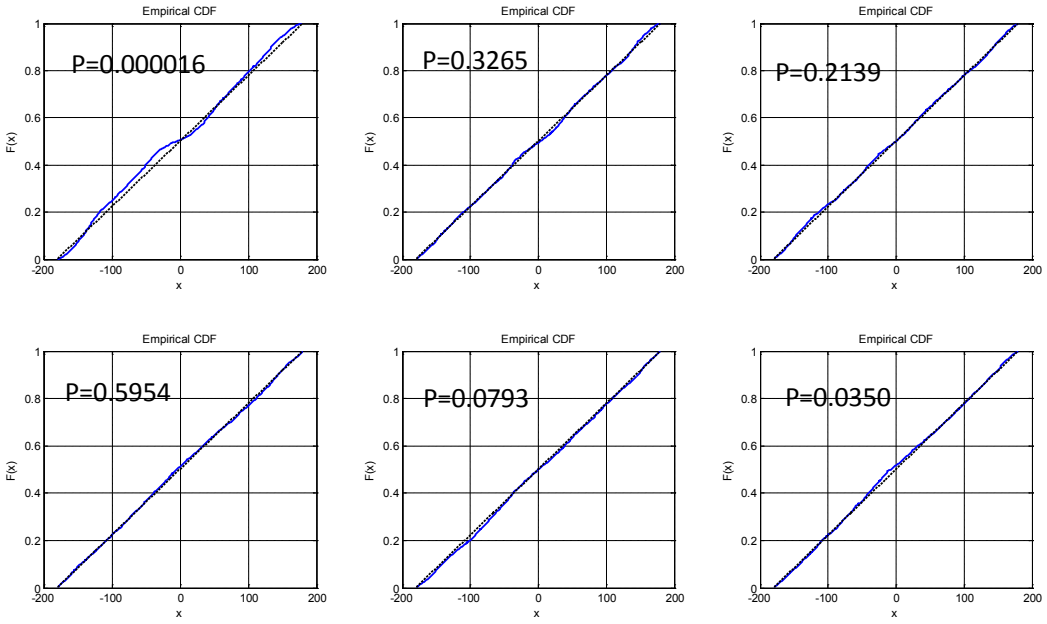

Figure 5. A comparison of empirical and uniform cumulative distribution functions for the nearest neighbors (1^{st}-3^{rd} neighbors are from left to right on the top row; 4^{th}-6^{th} neighbors are from left to right on the bottom row. The p-value is shown for each (the null hypothesis is that the empirical data fit a uniform distribution).

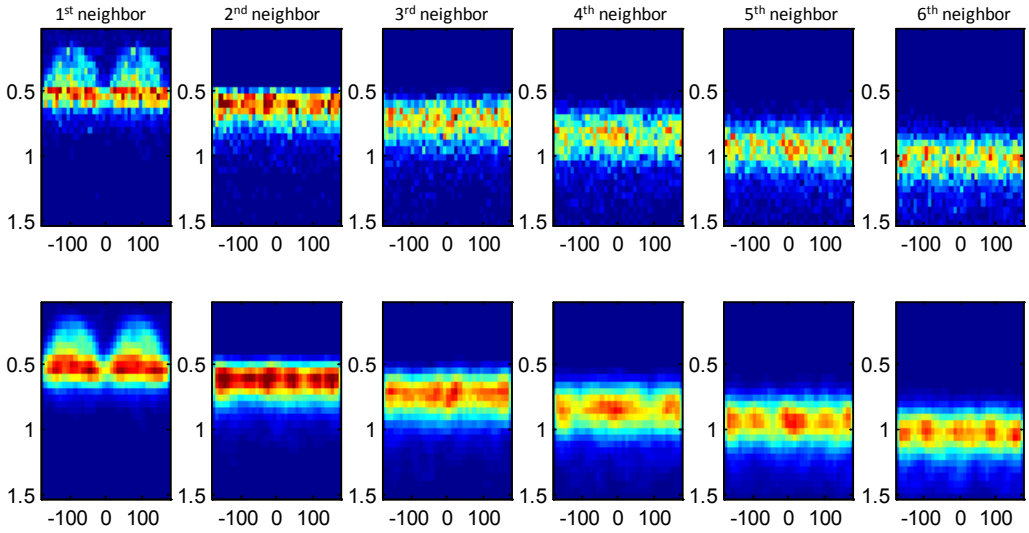

Figure 6. 2D histograms describing the positional dependency of the nearest neighbors of an individual tuna for simulated schools of tuna, using information describing the positional dependence of nearest neighbors only. (see Figure 4 for details).

RESULTS

Together, the multibeam data and the aerial imagery have been used to generate a school model that lends itself to Monte Carlo simulations. These models encompass the overall school shape, based on horizontal and vertical school cross sections derived from the aerial imagery and multibeam data, respectively, which results in an ellipsoidal school shape. The fish within the school are then seeded in three different ways: 1) according to a Poisson process, with no preferred location for any fish within the school; 2) with a 'hole correction' so that the 0.5 body length nearest neighbor location is preserved; and 3) with a higher degree of imposed order that preserves both the preferred nearest neighbor distance and the preferred relative bearing to the nearest neighbor. Although all three simulated school 'types' exhibit a high degree of randomness, imposing spatial correlation in both range and bearing to the nearest neighbors exhibits the most order in the simulated school (Figure 7).

For each of the three simulated cases, the frequency dependent target strength for CW waves (i.e., resolution cells considerably larger than the school size) is shown in Figure 8. Above the individual swimbladder resonance, the single scattering and multiple scattering differ by approximately 1-2 dB. Near resonance, the difference is more striking with a substantial downward shift in the school target resonance, indicating a collective oscillation of the school rather than a sum of individual oscillations. The imposed order within the school also changes the frequency dependent target strength, most notably for the case with both a preferred nearest neighbor distance and relative bearing. In this case, there appear to be two higher order school modes centered at approximately 1500 and 3000 Hz, which corresponds to wavelengths that are close to integer multiples of the individual fish spacing. The differences between the different school types is detectable but weak, with school target strength differences on the order of 1-2 dB above 1 kHz.

The model was also used to simulate the backscattered return from the school using a gated pulse (center frequency of 3 kHz, 2 kHz bandwidth, Hanning window applied to frequency spectrum). The resulting time series (i.e., as the pulse sweeps across the school) shows a nearly constant target strength (-37 dB) from the school and a scintillation index, $\langle I^2 \rangle / \langle I \rangle^2 - 1$, that is equal to one except on the school edges where it becomes quite high (likely due to the random appearance of small numbers of fish on the school edges). The resulting pdf of backscatter echo amplitudes, corresponding to a point within the center of the backscattered return from the school, fit Weibull distributions (Figure 10).

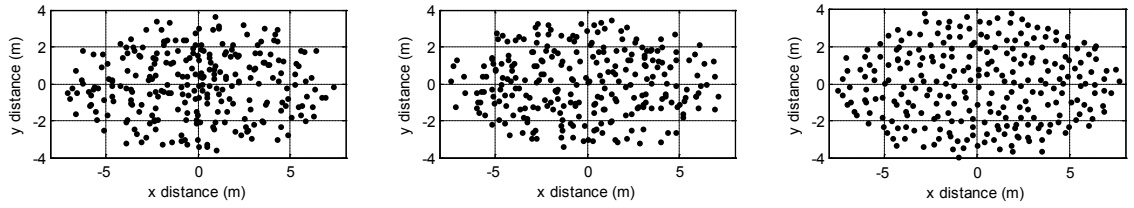

Figure 7. Examples of the simulated schools. Left: no spatial order (Poisson distributed). Middle: preferred nearest neighbor criteria. Right: preferred nearest neighbor and relative bearing criteria.

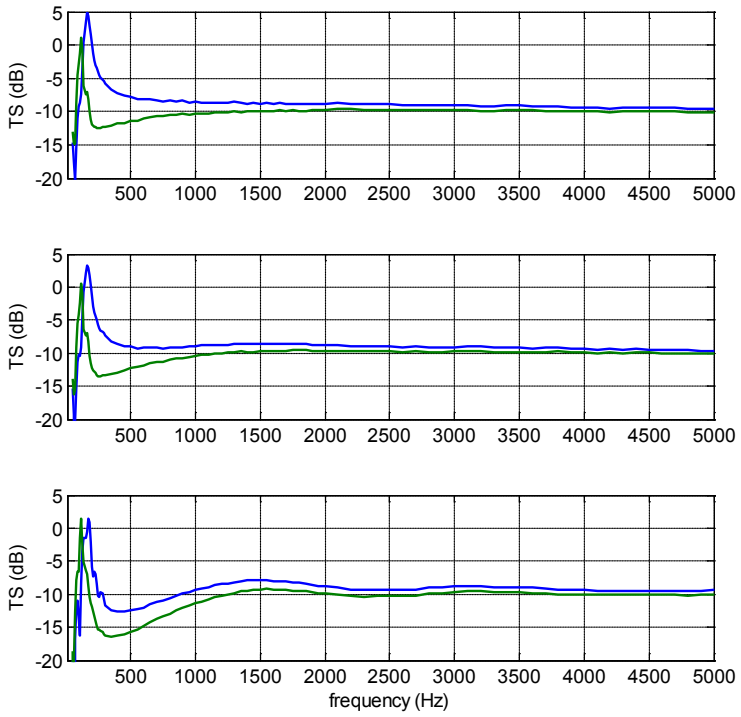

Figure 8. Average school target strength for simulated schools, CW insonification. Top: Poisson distributed; Middle: Preferred nearest neighbor distance; Bottom: Preferred nearest neighbor distance and bearing. In each case, the blue line is the single scatter solution and the green line is the multiple scatter solution.

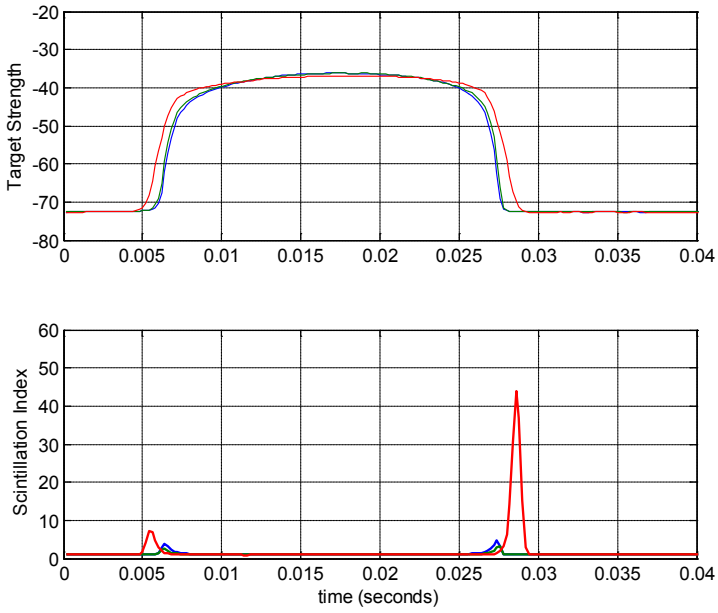

Figure 9. Top: Average school target strength for simulated schools, 2 kHz bandwidth pulse insonification. Bottom: the scintillation index for the simulated schools. Blue line: Poisson distributed; Green line: Preferred nearest neighbor distance; Red line: Preferred nearest neighbor distance and bearing.

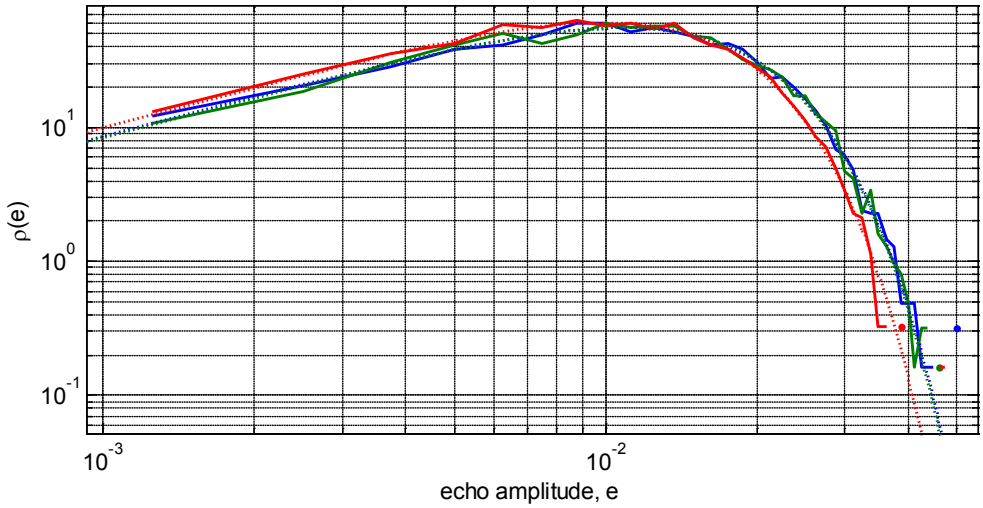

Figure 10. Probability density function of simulated echo amplitudes for Poisson distributed (blue), preferred nearest neighbor (green), and preferred nearest neighbor and relative bearing (red). Fitted Weibull distributions are shown as the dashed lines.

IMPACT/APPLICATIONS

Accurate predictions of reverberation from schools of fish (both mean levels and higher order statistical moments) serve the community of scientists and engineers tasked with developing active sonar systems, increasing their ability to design hardware (e.g., select frequencies, system topologies for multi-static sensors, etc.), develop signal processing algorithms aimed at detection/classification/ localization/tracking, estimate system performance, and design realistic sonar simulations. Generating realistic models of fish schools and the reverberation associated with them is challenging, primarily because data describing the fish schools themselves is often lacking or under-sampled. This work has exploited high resolution multibeam data and aerial imagery of Atlantic bluefin tuna – a bioclutter candidate – to generate an accurate school model that includes spatial structure within the fish school. In turn, this model has been used to examine the implications of this spatial structure on important modeling/simulation/data interpretation questions such as whether multiple scattering is important or can be neglected, whether school collective resonances are present, and what distributions echo amplitudes can be expected to follow.

RELATED PROJECTS

Acoustic assessment of juvenile bluefin tuna aggregations: a feasibility study. PI: Molly Lutcavage, UNH. Sponsor: Northeast Consortium.

REFERENCES

Foldy, L., The multiple scattering of waves, *Phys. Rev.* 67, 107-119, 1945.

Gibbs and Collette, Comparative anatomy and systematic of the tunas, GENUS THUNNUS, *Fish. Bull.* 66, 65-131, 1966.

Love, R., Resonant acoustic scattering by swimbladder-bearing fish, *J. Acoust. Soc. Am.*, 64, 571-580, 1978.

Magnuson, J.J., Comparative study of adaptation for continous swimming and hydrostatic equilibrium of scombroid and xiphoid fishes, *US Fish. Bull.* 71, 337-356, 1973.

Schaefer, K., and C. Oliver, Shape, volume, and resonance frequency of the swimbladder of yellowfin tuna, *Thunnus albacores, Fish. Bull.* 98, 364-374, 2000.

Weber, T., A. Lyons, D. Bradley, Acoustic propagation through bubble clouds exhibiting spatial structure in the fluctuating number density, *IEEE J. Oceanic Eng.* **32**(2), 513-523, 2007.

Weber, T., Observations of clustering in oceanic bubble plumes and acoustic implications, *J. Acoust. Soc. Am.*, 124, 2783-2792, 2008